A threedimensional wave packet study of ArI2(B)→Ar + I + I electronic predissociation

Octavio Roncero, Nadine Halberstadt, and J. Alberto Beswick

Citation: J. Chem. Phys. **104**, 7554 (1996); doi: 10.1063/1.471655
View online: http://dx.doi.org/10.1063/1.471655
View Table of Contents: http://jcp.aip.org/resource/1/JCPSA6/v104/i19
Published by the American Institute of Physics.

A three-dimensional wave packet study of $Ar\cdots I_2(B)\rightarrow Ar + I + I$ electronic predissociation

Octavio Roncero
Instituto de Matemáticas y Física Fundamental, CSIC, Serrano 123, 28006 Madrid, Spain

Nadine Halberstadt and J. Alberto Beswick
Laboratoire de Collisions, Agrégats et Réactivité, IRSAMC, Université Paul Sabatier, 31062 Toulouse, France

(Received 27 October 1995; accepted 6 February 1996)

A three-dimensional wave packet study of $Ar\cdots I_2(B)\rightarrow Ar + I(^2P_{3/2}) + I(^2P_{3/2})$ electronic predissociation, arising from the argon-induced electrostatic coupling between the $B(^3\Pi_{0^+u})$ and the repulsive $a(^3\Pi_{1g})$ state of I_2, is presented. A time-dependent golden rule approach is used. The initial wave packet corresponds to a bound vibrational wave function of the $Ar\cdots I_2(B)$ complex (with zero total angular momentum) multiplied by the electronic coupling. A 3-D propagation in the final dissociative surface is then performed and the predissociation rates are obtained by Fourier transform of the wave packet autocorrelation function. The potential energy surfaces are described by sums of atom–atom interactions. For the $B(^3\Pi_{0^+u})$ state potential, empirically determined van der Waals parameters available from the literature are used. For the final dissociative $a(^3\Pi_{1g})$ electronic state, the van der Waals parameters are adjusted to reproduce the experimentally observed oscillations of the electronic predissociation rate as a function of the initial vibrational quantum number v' of I_2. It is shown that good agreement between calculated and measured values can be obtained with a van der Waals well of 100 cm^{-1} and an interstate coupling of the order of 14 cm^{-1}. © *1996 American Institute of Physics.* [S0021-9606(96)01018-4]

I. INTRODUCTION

One of the current goals in the field of chemical physics is to understand the role of weak intermolecular forces (solvation bonds) in chemical reactivity and relaxation. In this context, the iodine molecule has been studied extensively under a wide variety of experimental conditions in compressed gases and liquids.[1–9] It has been suggested that some of the dynamical processes observed in gases and condensed phases could actually be due to the formation of van der Waals complexes between I_2 and the solvent particles. These complexes can be studied with the use of supersonic beams, and a large number of experimental and theoretical studies have been devoted to the study of the excitation and decay of van der Waals complexes involving I_2.[10–14]

When the van der Waals molecule $M\cdots I_2$, where M is a rare gas atom or a molecule, is excited in the spectral region of the $I_2(B\leftarrow X)$ transition, the fluorescence excitation spectrum shows broadened features which are attributed to quasibound levels associated to $M\cdots I_2(B,v')$. These resonances can decay by vibrational predissociation (VP),

$$M\cdots I_2(B,v')\overset{VP}{\rightarrow} M+I_2(B,v\leqslant v') \tag{1}$$

and/or by complex-induced electronic predissociation (EP),

$$M\cdots I_2(B,v')\overset{EP}{\rightarrow} M+I(^2P_{3/2})+I(^2P_{3/2}) \tag{2}$$

Since channel 1 produces electronically excited I_2 fragments which can fluoresce while channel 2 is dark, measurements of the $M\cdots I_2$ absorption/I_2 fluorescence quantum yield ratio in conjunction with absorption spectra can provide the relative importance of vibrational and electronic predissociation.[13] For $He\cdots I_2$ and $Ne\cdots I_2$, vibrational predissociation is much faster than electronic predissociation. For $Kr\cdots I_2$ on the other hand, electronic predissociation seems to dominate because fluorescence from excitation of the discrete $B\leftarrow X$ bands seen in absorption is completely quenched.[11]

For $Ar\cdots I_2$ the relative importance of vibrational and electronic predissociation depends very much on the vibrational quantum number v' of the initially excited state.[10,11,13] For low vibrational levels ($v'<15$) electronic predissociation prevails, but for highly excited levels ($v'>30$) vibrational predissociation dominates. In the range $15<v'<30$, where the two channels compete, it was found[10,13] that the electronic predissociation rates oscillate as a function of v', and that these oscillations are similar to those observed in the electric-field-induced quenching of the B state of isolated I_2.[15] This suggests that the repulsive potential energy surface responsible for the complex-induced electronic predissociation, channel 2, is the same as the one involved in the electric-field-induced predissociation.[15–17] The state responsible for this quenching is believed to be the $a(^3\Pi_{1g})$ state (see Fig. 1).

The simplest approach to this problem is to consider the argon atom as a spectator, providing the electronic coupling between the $B(^3\Pi_{0^+u})$ and $a(^3\Pi_{1g})$ states of I_2 but not taking part into the dynamics. The electronic predissociation rates are then simply proportional to the bound-continuum Franck–Condon factors between the wave functions of I_2 in the two states. A calculation using this model was performed.[18] The results showed very clearly that the Franck–Condon factors for transitions from v' in the range

 0021-9606/96/104(19)/7554/7/$10.00

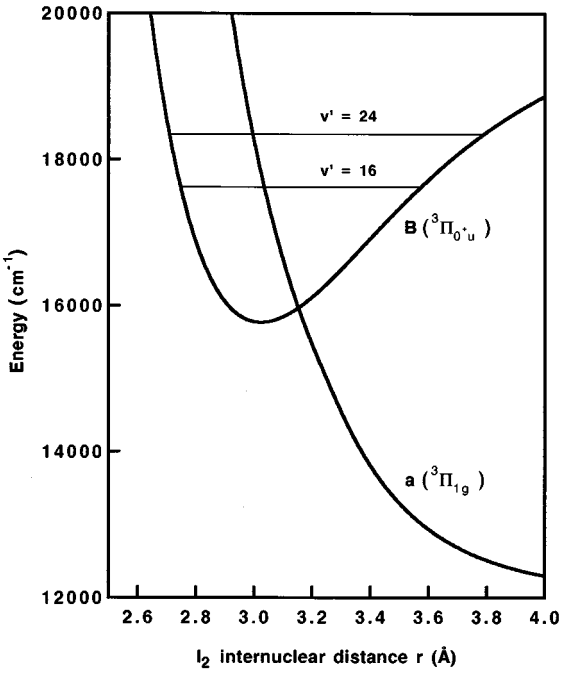

FIG. 1. $B(^3\Pi_{0^+u})$ and $a(^3\Pi_{1g})$ potential curves of I_2. The $B(^3\Pi_{0^+u})$ curve is calculated from a fit [Eq. (7)] to literature data (see Refs. 16, 23–25). The $a(^3\Pi_{1g})$ is taken from Ref. 16. The calculations in this work are for $16<v'<24$. Levels $v'=16$ and 24 are represented in the B curve.

$v'=16$–24 to the $a(^3\Pi_{1g})$ state oscillate much the same as the experimental electronic predissociation rates. This is in contrast with what was found for the other candidate, the $B''(^1\Pi_{1u})$ electronic state of I_2, which in this range gives a smooth variation of the Franck–Condon factors. An improved agreement between $B-a$ Franck–Condon factors and electronic predissociation rates can be obtained by observing that the argon atom, in addition to inducing the coupling, also shifts the I_2 potential curves. Good agreement was obtained for two different shifts of the final $a(^3\Pi_{1g})$ state: -100 cm^{-1} and $+900$ cm^{-1}.[18]

In the calculations mentioned above, the dynamics of the dissociating argon atom was completely neglected. Recently,[19] a two-dimensional wave packet calculation was performed to study the effect of the argon atom dynamics. Ar···I_2 was assumed to be fixed in the T-shaped configuration and two different van der Waals potentials were tested for the $a(^3\Pi_{1g})$ state: one was attractive giving a shift of -100 cm^{-1} at the equilibrium geometry, and the other repulsive giving a shift of $+900$ cm^{-1}. For the attractive potential it was found that the results were essentially those of the Franck–Condon model. On the other hand, for the repulsive van der Waals interaction the oscillations of the electronic predissociation rate were washed out by the rapid dephasing of the initial wave packet due to the departure of the Ar atom. Thus it was concluded that the motional state of the departing Ar atom is very important in this process.

Since these calculations were performed with the Ar atom restricted to move on a line perpendicular to the I–I bond, it was necessary to perform a full three-dimensional treatment to check this approximation. It is the purpose of this paper to present the results of such a calculation. Since Eq. (2) corresponds to a three-body fragmentation process, it is quite difficult to treat this problem by the usual time-independent techniques. If box-quantization is used for one of the reaction coordinates for instance, the number of resulting coupled equations to integrate is very large. An alternative method involves the wave packet golden rule method which has been used before to treat vibrational predissociation in van der Waals molecules.[20,21] In Sec. II we present the methodology and the input parameters for the calculations. Section III presents the results and their discussion. Finally, Sec. IV is devoted to the conclusions.

II. THEORETICAL METHOD

In the framework of the time-dependent golden rule approach,[20,21] an initial wave packet is defined by the product of the quasibound wave function $|\phi_0\rangle$ with the coupling matrix element V_c responsible for predissociation,

$$|\Phi(t=0)\rangle = V_c|\phi_0\rangle/N, \tag{3}$$

where N is the normalization constant of the wave packet

$$N=\sqrt{\langle\phi_0|V_c^2|\phi_0\rangle}. \tag{4}$$

It can then be shown that the half-width (HWHM) Γ of the resonance associated to the initial quasibound level $|\phi_0\rangle$ is given by

$$\Gamma(E)=\frac{\langle\phi_0|V_c^2|\phi_0\rangle}{2\hbar}\left(\int_0^\infty dt\ e^{iEt/\hbar}C(t)+\text{c.c.}\right) \tag{5}$$

calculated at the energy E_0 of $|\phi_0\rangle$. In Eq. (5)

$$C(t)\equiv\langle\Phi(t=0)|\Phi(t)\rangle \quad \text{with} \quad |\Phi(t)\rangle=e^{-iH_dt}|\Phi(t=0)\rangle \tag{6}$$

is the autocorrelation function of the wave packet evolving in the final dissociative state described by the Hamiltonian H_d. From Eq. (5), the predissociation rate k can be obtained using $k=2\Gamma/\hbar$.

In this work we study the process of electronic predissociation in Ar···I_2 as written in Eq. (2). The initial quasibound state is chosen to be the zero-point van der Waals level of the complex with I_2 in the $B(^3\Pi_{0^+u})$ electronic state and vibrational level v'. This corresponds to the actual conditions of the experiments.[13]

The final dissociative state is Ar···$I_2[a(^3\Pi_{1g})]$, which correlates asymptotically to the Ar + I($^2P_{3/2}$)+ I($^2P_{3/2}$) limit. Between the $B(^3\Pi_{0^+u})$ and the $a(^3\Pi_{1g})$ states of I_2, there is an electrostatic coupling induced by the presence of the argon atom, which is maximum for the T-shape configuration. In the colinear configuration this coupling vanishes since the two states have different projection Ω_e of the electronic angular momentum (orbital + spin) on the I_2 axis, $\Omega_e[B(^3\Pi_{0^+u})]=0$ while $\Omega_e[a(^3\Pi_{1g})]=1$. For Ar···$I_2$ the vibrational predissociation channel in Eq. (1) is mediated by intramolecular vibrational relaxation between the initial v' state and highly excited bending levels in the v'-1 and v'-2 manifolds.[22] Since the electrostatic coupling between

TABLE I. Potential parameters for the $I_2 B(^3\Pi_{0^+u})$ [Eq. (7)] and $a(^3\Pi_{1g})$ [Eq. (8)] states and for the van der Waals interaction in the B [Eq. (10)] state and in the a state, attractive [Eq. (11)] and repulsive [Eq. (12)] forms.

$V_B(r)$ Eq. (7)	$V_a(r)$ Eq. (8)	
$T_e = 15\,769$ cm^{-1}	$\epsilon = 140$ cm^{-1}	
$\omega_e = 125.69$ cm^{-1}	$W = 12\ 547$ cm^{-1}	
$\omega_e\chi_e = 0.764$ cm^{-1}	$A_1 = 3.455 \times 10^8$ cm^{-1} Å^{10}	
$r_e = 3.024$ Å	$A_2 = 131$ cm^{-1}	
$V_B(\infty) = 20\ 150$ cm^{-1}	$A_3 = 4.212 \times 10^9$ cm^{-1} Å^{12}	
$r_s = 3.28$ Å	$A_4 = 487.5$ cm^{-1}	
V_{ArI}[a] Eq. (10)	$V_{\mathrm{ArI}}^{\mathrm{attr.}}$ Eq. (11)	$V_{\mathrm{ArI}}^{\mathrm{rep.}}$ Eq. (12)
$D = 122$ cm^{-1}	$D^{\mathrm{attr.}} = 50$ cm^{-1}	$D^{\mathrm{rep.}} = 450$ cm^{-1}
$\alpha = 1.3228$ Å^{-1}	$\alpha = 1.3228$ Å^{-1}	$\alpha = 1.3228$ Å^{-1}
$\overline{R}_{\mathrm{ArI}} = 4.2$ Å	$\overline{R}_{\mathrm{ArI}} = 4.2$ Å	$\overline{R}_{\mathrm{ArI}} = 4.2$ Å

[a]References 26 and 27.

the $B(^3\Pi_{0^+u})$ and the $a(^3\Pi_{1g})$ states is zero for the linear configuration, highly excited bending levels should be very weakly coupled to $a(^3\Pi_{1g})$. Hence, we assume that electronic predissociation is dominated by the coupling between the initial zero-point van der Waals level of the v' manifold and the final dissociative continuum of the $a(^3\Pi_{1g})$ state, with no interference between vibrational predissociation and electronic predissociation.

The potential energy surfaces for the initial and final states are modeled by a sum of pairwise functions. The I_2 potential energy curves for the $B(^3\Pi_{0^+u})$ and $a(^3\Pi_{1g})$ electronic states are taken from the literature.[16,23–25] The $I_2[B(^3\Pi_{0^+u})]$ potential is adjusted to a Morse plus a long range interaction according to:

$$V_B(r) = \begin{cases} T_e + D_{I_2}(1 - e^{-\alpha_{I_2}(r-r_e)})^2 & r \leqslant r_s \\ V_B(\infty) - C_6/r^6 - C_8/r^8 - C_{10}/r^{10} & r > r_s \end{cases} \tag{7}$$

with $D_{I_2} = \omega_e^2/4\omega_e\chi_e$ and $\alpha_{I_2} = \sqrt{2\mu\omega_e}/\hbar$, μ being the reduced mass of I_2 taken equal to 63.452 amu. The numerical values for the parameters are given in Table I. C_6, C_8, and C_{10} are determined by continuity of the potential and its first and second derivatives at the switching point $r_s = 3.28$ Å. As for the $I_2[a(^3\Pi_{1g})]$ potential we use the form[16]

$$V_a(r) = \tfrac{1}{2}[U_m(r) + U_p(r) - \sqrt{(U_m(r) - U_p(r))^2 + \epsilon^2}] + W \tag{8}$$

with

$$U_m(r) = \frac{A_1}{r^{10}} - A_2; \quad U_p(r) = \frac{A_3}{r^{12}} - A_4. \tag{9}$$

The parameters in Eqs. (8) and (9) are also collected in Table I.

The individual van der Waals Ar···I potentials for the $B(^3\Pi_{0^+u})$ state are represented by Morse functions

$$V_{\mathrm{ArI}}(R_{\mathrm{ArI}}) = D\{e^{-2\alpha(R_{\mathrm{ArI}} - \overline{R}_{\mathrm{ArI}})} - 2e^{-\alpha(R_{\mathrm{ArI}} - \overline{R}_{\mathrm{ArI}})}\} \tag{10}$$

with parameters determined by Gray[26,27] from a fitting of structural data, such as equilibrium geometry and dissociation energy, as well as from vibrational predissociation data. The parameters are given in Table I. The potential in the $B(^3\Pi_{0^+u})$ electronic state has its minimum at the T-shaped configuration with the Ar atom at a distance of $R_e = 3.92$ Å from the center of mass of I_2. The energy of the van der Waals minimum is -244 cm^{-1} with respect to the dissociation limit.

As for the Ar···I interaction in the $a(^3\Pi_{1g})$ state, two different potentials have been used

$$V_{\mathrm{ArI}}^{\mathrm{attr.}}(R_{\mathrm{ArI}}) = D^{\mathrm{attr.}}\{e^{-2\alpha(R_{\mathrm{ArI}} - \overline{R}_{\mathrm{ArI}})} - 2e^{-\alpha(R_{\mathrm{ArI}} - \overline{R}_{\mathrm{ArI}})}\}, \tag{11}$$

$$V_{\mathrm{ArI}}^{\mathrm{rep.}}(R_{\mathrm{ArI}}) = D^{\mathrm{rep.}} e^{-2\alpha(R_{\mathrm{ArI}} - \overline{R}_{\mathrm{ArI}})}. \tag{12}$$

The values of the parameters are given in Table I. The values of $D^{\mathrm{attr.}}$ and $D^{\mathrm{rep.}}$ are those used in the spectator model,[18] the other parameters being equal to those of the $B(^3\Pi_{0^+u})$ state. Both forms gave electronic predissociation rate oscillations as a function of v' in good agreement with the measurements of Burke and Klemperer.[13]

Finally, for the coupling matrix element V_c between the $B(^3\Pi_{0^+u})$ and $a(^3\Pi_{1g})$ electronic states induced by the Ar atom, the form that was used in the previous 2D simulations[19] was taken as depending only on the distance between Ar and the center of mass of I_2

$$V_c(R) = Ae^{-\alpha R} \tag{13}$$

with the same $\alpha = 1.3228$ Å^{-1} parameter as used for the potentials in Eqs. (10), (11), and (12). The parameter A has been adjusted in order to fit exactly the experimental rate for $v' = 20$. This gives $A = 2490$ cm^{-1}. Thus in the region of the equilibrium geometry of the initial bound state ($R = R_e = 3.92$ Å), the electronic coupling is of the order of 14.0 cm^{-1}. The form we use in this work is taken from second-order perturbation theory for the electrostatic coupling[28]

$$V_c = \frac{A'}{R^7} \sin\theta\,(4\cos^2\theta - 1), \tag{14}$$

where R is the coordinate from the center of mass of I_2 to Ar, and θ the angle between R and the I_2 coordinate. In the colinear configuration this coupling goes to zero as it should (see above). A' is also adjusted in order to fit exactly the experimental rate for $v' = 20$, which gives $A' = 201.5 \times 10^3$ cm^{-1} in the case of the attractive van der Waals interaction in the $a(^3\Pi_{1g})$ state, and $A' = 266 \times 10^3$ cm^{-1} in the case of the repulsive form. In the region of the equilibrium geometry of the initial quasibound state, the electronic coupling is of the order of 14.2 and 18.8 cm^{-1} for the attractive and repulsive Ar–I interactions in the a state, respectively. Both forms for the electronic coupling are taken to be independent of r. The actual dependence of V_c in r should not affect the dynamics, since the $a(^3\Pi_{1g})$ and $B(^3\Pi_{0^+u})$ curves cross at a very acute angle hence the transition should be very localized around the crossing point.

The calculation is performed as follows. The total angular momentum is taken to be zero. For the initial quasibound state, the wave function is written as

$$\phi_0(r,R,\theta) = \chi_{v'}(r) F_{v'}(R,\theta), \tag{15}$$

where r is the I_2 internuclear coordinate, R the distance between the argon atom and the center of mass of I_2, and θ the angle between the two vectors **r** and **R**. In Eq. (15), the $\chi_{v'}(r)$ functions are the vibrational eigenfunctions of free I_2 in the $B(^3\Pi_{0^+u})$state. The van der Waals vibrational functions $F_{v'}(R,\theta)$ are obtained by diagonalizing the total Hamiltonian in a product basis set of 25 harmonic oscillator wave functions for R and 30 Legendre polynomials for θ. The frequency (30 cm^{-1}) and equilibrium distance (4.05 Å) of the harmonic oscillator functions are adjusted to the bottom of the van der Waals well. Only the zero-point van der Waals level is considered in this work.

The time evolution of the wave packet is calculated by a Lanczos procedure[29,30] using 15 Krylov functions with a time step of 0.1 fs. Multiplying the wave packet by $(rR\sin^{1/2}\theta)$, the Hamiltonian in the final dissociative state is

$$H_d = -\frac{\hbar^2}{2\mu}\frac{\partial^2}{\partial r^2} - \frac{\hbar^2}{2m}\frac{\partial^2}{\partial R^2} + \left\{\frac{\hbar^2}{2\mu r^2} + \frac{\hbar^2}{2mR^2}\right\}\frac{\partial^2}{\partial\theta^2} - \left\{\frac{\hbar^2}{2\mu r^2} + \frac{\hbar^2}{2mR^2}\right\}\left\{\frac{1}{2} + \frac{1}{4\tan^2\theta}\right\} + V_a(r) + W_a(r,R,\theta) \tag{16}$$

where $\mu = M_I/2$, $m = M_{Ar}M_{I_2}/(M_{Ar}+M_{I_2}) = 34.554$ amu, and $W_a = V_{Ar\cdots I_1} + V_{Ar\cdots I_2}$ is the van der Waals potential in the final $a(^3\Pi_{1g})$ state. The action of the kinetic terms involving second derivatives in Eq. (16) is evaluated using the FFT method.[31] The calculations are performed on a grid of 512 points in r from 2.2 to 7.5 Å, 64 points in R from 3.0 to 6.0 Å, and 32 values in θ around the T-shaped configuration (from $\pi/3$ to $2\pi/3$). Absorption along r is performed starting from $r = 6.0$ Å as follows. The fraction of the wave packet that is in the absorbing region is multiplied by the decaying part of a Gaussian with exponential parameter 0.025 $Å^{-1}$. The absorbed probability is monitored using the method of Pernot and Lester,[32] in order to check for the conservation of the norm of the wave packet during evolution. No absorption was needed in R nor in θ as the wave packet never reached the edge of the grid in these coordinates.

III. COMPARISON WITH EXPERIMENTS

The calculations are performed for initial states of Ar··· I_2(B,v') in the range $v' = 16$–24 corresponding to the experiments by Burke and Klemperer.[13]

In Figs. 2 and 3, we present snapshots of the time evolution of the wave packet probability density along the I_2 internuclear distance r

$$P(r;t) = \int dR\, d\theta\, |\Phi(r,R,\theta;t)|^2 \tag{17}$$

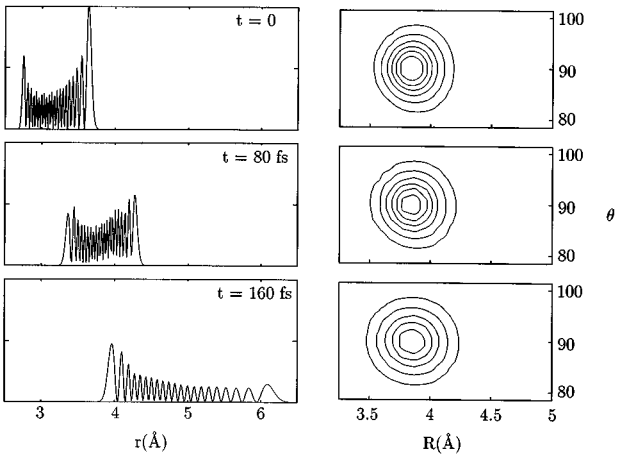

FIG. 2. Snapshots of the wave packet probability density projected along the I_2 coordinate r (left-hand side) and van der Waals coordinates R and θ (right-hand side), for the attractive form of the van der Waals interaction in the $a(^3\Pi_{1g})$ state [Eq. (11)]. The initial state corresponds to $v' = 20$.

with $\int dr\, P(r;t) = 1$, and two-dimension contour plots of the wave packet probability density along the van der Waals coordinates R and θ

$$P(R,\theta;t) = \int dr |\Phi(r,R,\theta;t)|^2 \tag{18}$$

with $\int dR\, d\theta\, P(r;t) = 1$ (note that since the wave packet has been multiplied by $(rR\sin^{1/2}\theta)$, the total volume element is $dV = dr\, dR\, d\theta$). The initial ($t = 0$) wave packet corresponds to Ar···I_2(B, $v' = 20$). Figure 2 is for the attractive form of Eq. (11) of the van der Waals interaction in the $a(^3\Pi_{1g})$ state, while Fig. 3 corresponds to the repulsive form of Eq. (12). The results are presented for the coupling of Eq. (14), but they are essentially indistinguishable from the results obtained with the coupling of Eq. (13) that we previously used in two-dimensional calculations. From a cursory examination of Figs. 2 and 3 it is clear that the motion along the I_2 internuclear distance is very fast and that the dissocia-

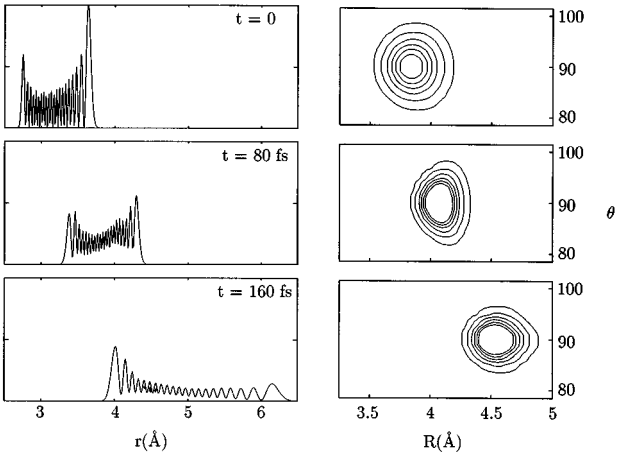

FIG. 3. Snapshots of the wave packet probability density projected along the I_2 coordinate r (left-hand side) and van der Waals coordinates R and θ (right-hand side), for the repulsive form of the van der Waals interaction in the $a(^3\Pi_{1g})$state [Eq. (12)]. The initial state corresponds to $v' = 20$.

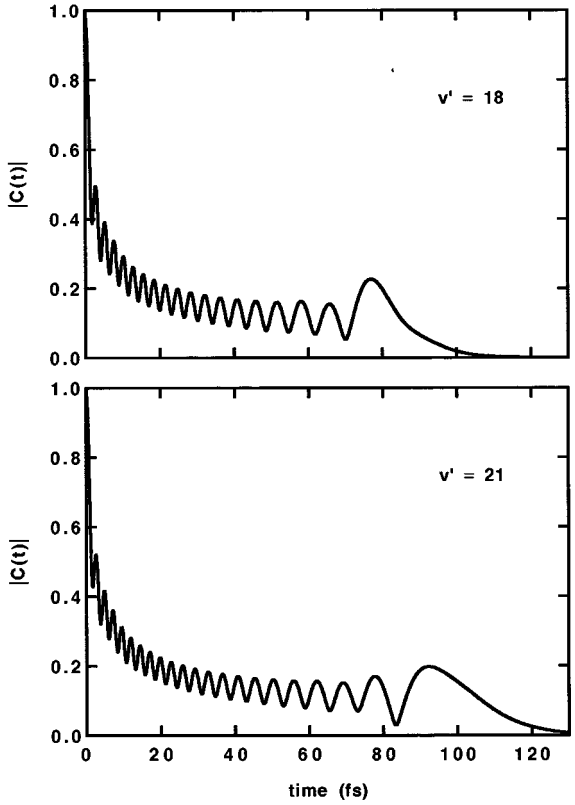

FIG. 4. Autocorrelation function [Eq. (6)] of the $Ar\cdots I_2$ wave packet evolving in the final dissociative state with an attractive van der Waals interaction [Eq. (11)]. The initial quasibound states are $v'=18$ and 21.

tion is essentially finished in about 100 fs. During that time the dynamics of the argon atom depends on the nature of the potential in the $a(^3\Pi_{1g})$ state. In the case of the attractive form, Fig. 2, the argon atom remains stationary, experiencing only a slight force towards the middle point between the two iodine atoms. Thus it behaves as a ''spectator,'' only providing the coupling between the B and a states of I_2 leading to electronic predissociation. In the case of a repulsive Ar–I interaction in the $a(^3\Pi_{1g})$ state (Fig. 3), the argon atom clearly moves away during the dissociation of I_2 and can no longer be considered as a spectator.

Figure 4 presents the autocorrelation function $C(t)$, Eq. (6), for two different initial vibrational levels of I_2 ($v'=18$ and 21), for the attractive a state van der Waals interaction. As expected from the behavior of the wave packet represented in Fig. 2, the autocorrelation function decreases very fast in a time of the order of 100 fs. This rapid decay is modulated by oscillations corresponding to the overlapping or antioverlapping of the maxima of the initial I_2 wave function with the evolving wave packet.

In contrast, the autocorrelation function for the repulsive a state van der Waals interaction decreases faster. This can be seen in Fig. 5, which presents the autocorrelation function for the initial vibrational level $v'=20$ of I_2. The oscillations that were present in Fig. 4 are now damped. This is due to the motion of the Ar atom that was visible in Fig. 3. This was also observed in the two-dimensional calculation[19] and explained why the electronic predissociation rates did not oscillate as a function of v' for this form of van der Waals interaction in the a state.

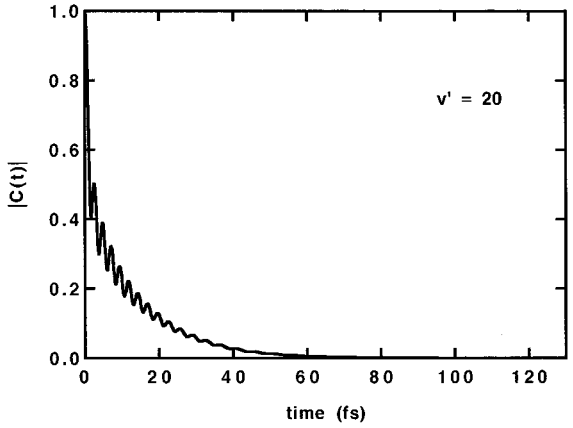

FIG. 5. Autocorrelation function [Eq. (6)] of the $Ar\cdots I_2$ wave packet evolving in the final dissociative state with a repulsive van der Waals interaction [Eq. (12)]. The initial quasibound state is $Ar\cdots I_2$ (B,$v'=20$).

In Fig. 6 we present a plot of the function $\Gamma(E)$ of Eq. (5), which is proportional to the Fourier transform of the autocorrelation function presented in Fig. 4. The$Ar\cdots I_2$ complex was initially in the (B, $v'=18$) state, and the van der Waals interaction in the a state is attractive. The value of $\Gamma(E)$ at the energy E_0 of the initial quasibound level provides the half-width Γ of the resonance [see Eq. (5)] and the rate $k=2\Gamma/\hbar$ for electronic predissociation. Since $\Gamma(E)$ oscillates rapidly, it is expected that the electronic predissociation rates will oscillate as a function of v'.

Figure 7 presents the $\Gamma(E)$ function for the repulsive form of the van der Waals interaction in the a state, when the $Ar\cdots I_2$ complex is initially excited to the $v'=20$ level. It can

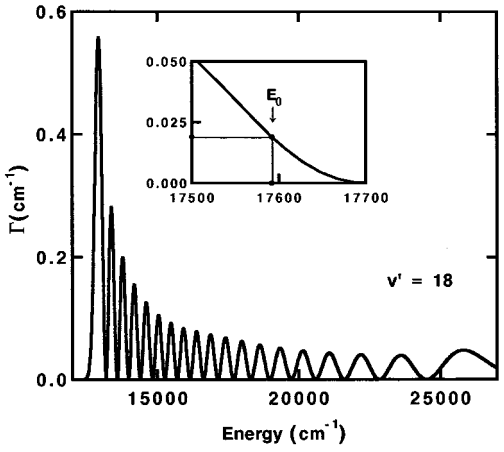

FIG. 6. $\Gamma(E)$ [Eq. (5)] of the $Ar\cdots I_2$ wave packet evolving in the final dissociative state with an attractive van der Waals interaction [Eq. (11)], for the initial quasibound states $v'=18$. Shown as an inset is a zoom around the energy E_0 of the quasibound state, the electronic predissociation linewidth being given by the value of $\Gamma(E_0)$.

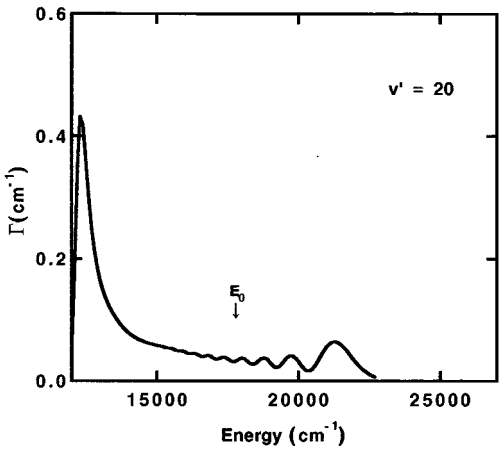

FIG. 7. $\Gamma(E)$ [Eq. (5)] of the $Ar\cdots I_2$ wave packet evolving in the final dissociative state with a repulsive van der Waals interaction [Eq. (12)], for the initial quasibound states $v'=20$. The arrow points at the energy E_0 of the quasibound state, the electronic predissociation linewidth is given by the value of $\Gamma(E_0)$.

be seen that $\Gamma(E)$ has far fewer oscillations, hence it can be expected that the electronic predissociation rates will be smooth as a function of v'.

In Fig. 8 we present all the calculated rates together with the experimental results of Burke and Klemperer.[13] As stated above, the strength of the interstate coupling has been fitted so that the calculated rate for $v'=20$ be equal to the experimental value. Also, the energy minimum of the van der Waals interaction in the final $a(^3\Pi_{1g})$ state has been very roughly adjusted[18] (by steps of 100 cm^{-1}) in order for the $v'=20$ rate to be a maximum. From this figure the repulsive form of the van der Waals interaction in the a state can be ruled out since the variation of the electronic predissociation rate does not present the oscillations of the experimental one.

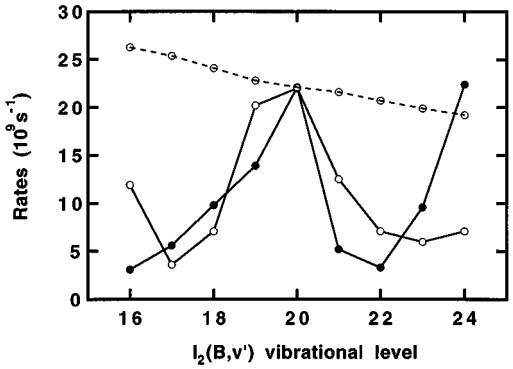

FIG. 8. Calculated versus experimental rates $k=2\Gamma/\hbar$ for the electronic predissociation of $Ar\cdots I_2$ $B(^3\Pi_{0^+u})$, $v'=16$–24. The results were scaled (see the text) such that the electronic predissociation linewidth coincide with the experimental one for $v'=20$. The black dots represent the experimental data of Burke and Klemperer (Ref. 13). The empty dots represent the results of the three-dimensional calculations for electronic predissociation by the $a(^3\Pi_{1g})$ state. The continuous and the dashed lines correspond to an attractive and a repulsive van der Waals interaction in the a state, respectively.

TABLE II. Comparison between two-dimensional (Ref. 19) and three-dimensional (this work) results.

Attractive		
v	2D	3D
18	0.034	0.034
20	0.102	0.100
21	0.054	0.056
	Repulsive	
v	2D	3D
20	0.059	0.058
21	0.056	0.056

On the other hand, the attractive form of the van der Waals interaction in the a state gives oscillations that are very similar to the experimental ones. Considering the simplicity of the model and the fact that no other potential parameter (such as the exponential repulsive parameter α) has been varied, the agreement between calculated and experimental rates can be considered as good.

The conclusions from Fig. 8 are very similar to those obtained in the two-dimensional calculation.[19] In Table II, the results obtained in this work for $v=18$, 20, and 21 (for the repulsive form of the a state van der Waals interaction) and for $v=20$ and 21 (for the repulsive form) are compared with those obtained in the two-dimensional calculation of Ref. 19. In this table the rates have been divided by $\langle\phi_0|V_c^2|\phi_0\rangle$, since V_c and ϕ_0 are not the same in the 2D and 3D calculations. This table shows that the dynamics in the final dissociative surface are very similar. This can be due to the fact that around the equilibrium T-shape configuration there is no torque in the a state (since for the attractive form this configuration also corresponds to a minimum), and that the rotational period for the complex (about 84 ps around the equilibrium configuration) is much longer than the time it takes for I_2 to dissociate. This is in agreement with the prediction of the sudden approximation.

IV. CONCLUSIONS

We have presented wave packet golden rule calculations for the electronic predissociation of $B(^3\Pi_{0^+u})$ state, $v'=16$–24, $Ar\cdots I_2$. It was assumed that the electronic state responsible for the predissociation is the repulsive $a(^3\Pi_{1g})$ state and that the coupling between the B and a states is induced by the presence of the Ar atom. While in press, we became aware of a very complete DIM study of the Ar–I_2 potential energy surfaces.[33] Qualitative arguments from these calculations indicate that although the B–B'' coupling seems to be more important at the T-shape configuration, as soon as the $Ar\cdots I_2$ angle θ departs slightly from $\pi/2$ ($\theta=85°$), the B–a coupling wins.

The oscillations of the electronic predissociation rates as a function of v' are well reproduced with a coupling of the order of 14 cm^{-1} and an attractive van der Waals potential in the final $a(^3\Pi_{1g})$ state with a well depth of 100 cm^{-1}.

From the calculations presented above it is clear that the $a(^3\Pi_{1g})$ state can satisfactorily describe electronic predissociation of $I_2(B)$–Ar complexes, as suggested by Burke and Klemperer.[13] It is then very likely that the $a(^3\Pi_{1g})$ state is also involved in the collision induced predissociation of the B state.[34–40]

Finally, the three-dimensional calculations do not modify qualitatively the results from the two-dimensional calculations.

ACKNOWLEDGMENTS

We acknowledge support from the CNRS for the use of the computing facilities at IDRIS, and the European Community for visiting support (SCT-CT91-0699). One of us (O.R.) was supported by a grant from DGICYT No. PB92-0053 and Comunidad Autónoma de Madrid No. 064/92. O.R. also thanks CICYT and CIEMAT for computer time at the CRAY-YMP in Madrid. N.H. and J.A.B. thank the Director of the MPB Department of CNRS for a grant, and the Région Midi-Pyrénées for support.

[1] J.-C. Dutoit, J. M. Zellweger, and H. van den Bergh, J. Chem. Phys. **78**, 1825 (1983).
[2] B. Otto, J. Schroeder, and J. Troe, J. Chem. Phys. **81**, 202 (1984).
[3] J. T. Hynes, Annu. Rev. Phys. Chem. **36**, 573 (1985).
[4] J. Schroeder and J. Troe, Annu. Rev. Phys. Chem. **38**, 163 (1987).
[5] A. L. Harris, J. K. Brown, and C. B. Harris, Annu. Rev. Phys. Chem. **39**, 341 (1988).
[6] R. Lingle Jr., X.Xu, S. Yu, H. Zhu, and J. B. Hopkins, J. Chem. Phys. **93**, 5667 (1990).
[7] Y. Yan, R. M. Whitnell, K. R. Wilson, and A. H. Zewail, Chem. Phys. Lett. **193**, 402 (1992).
[8] N. F. Scherer, L. D. Ziegler, and G. R. Fleming, J. Chem. Phys. **96**, 5544 (1992).
[9] N. F. Scherer, D. M. Jonas, and G. R. Fleming, J. Chem. Phys. **99**, 153 (1993).
[10] D. H. Levy, Adv. Chem. Phys. **47**, 323 (1981).
[11] N. Goldstein, T. L. Brack, and G. H. Atkinson, J. Chem. Phys. **85**, 2684 (1986).
[12] D. M. Willberg, M. Gutmann, J. J. Breen, and A. H. Zewail, J. Chem. Phys. **96**, 198 (1992).
[13] M. L. Burke and W. Klemperer, J. Chem. Phys. **98**, 6642 (1993); *ibid.* **98**, 1797 (1993).
[14] M. Ben-Nun, R. D. Levine, D. M. Jonas, and G. R. Fleming, Chem. Phys. Lett. **245**, 629 (1995).
[15] F. W. Dalby, C. D. P. Levy, and J. Vanderlinde, Chem. Phys. **85**, 23 (1984).
[16] J. Tellinghuisen, J. Chem. Phys. **82**, 4012 (1985).
[17] C. Teichteil and M. Pélissier, Chem. Phys. **180**, 1 (1994).
[18] O. Roncero, N. Halberstadt, and J. A. Beswick, Caging and nonadiabatic electronic transision in I_2–M complexes, in *Reaction Dynamics in Clusters and Condensed Phases*, edited by J. Jortner, R. D. Levine, and B. Pullmann (Kluwer Academic, Dordrecht, 1994), p. 73.
[19] O. Roncero, N. Halberstadt, and J. A. Beswick, Chem. Phys. Lett. **226**, 82 (1994).
[20] P. Villarreal , S. Miret-Artés, O. Roncero, G. Delgado, Barrio, J. A. Beswick, N. Halberstadt, and R. Coalson, J. Chem. Phys. **94**, 4230 (1991).
[21] D. H. Zhang, J. Z. H. Zhang, and Z. Bačić, J. Chem. Phys. **97**, 3149 (1992).
[22] S. K. Gray and O. Roncero, J. Phys. Chem. **99**, 2512 (1995).
[23] R. F. Barrow and K. K. Yee, J. Chem. Soc. Faraday Trans. 2 **69**, 684 (1973).
[24] J. M. Hutson, S. Gerstenkorn, P. Luc, and J. Sinzelle, J. Mol. Struct. **96**, 266 (1982).
[25] M. Grubele and A. H. Zewail, J. Chem. Phys. **98**, 883 (1993).
[26] S. K. Gray, Chem. Phys. Lett. **197**, 86 (1992).
[27] S. K. Gray, J. Chem. Soc. Faraday Discuss. **97**, 143 (1994).
[28] O. Roncero, N. Halberstadt, and J. A. Beswick (unpublished).
[29] C. J. Lanczos, J. Res. Natl. Bur. Stand. **45**, 255 (1950).
[30] C. Leforestier , R. H. Bisseling, C. Cerjean, M. D. Feit, R. Friesner, A. Guldberg, A. Hammerick, G. Jolicard, W. Karrlein, H. D. Meyer, N. Lipkin, O. Roncero, and R. Kosloff, J. Comput. Phys. **94**, 59 (1991).
[31] J. W. Cooley and J. W. Tukey, Math. Comput. **19**, 297 (1965).
[32] P. Pernot and W. Lester, Int. J. Quantum Chem. **40**, 577 (1991).
[33] A. A. Buchachenko and N. F. Stepanov (unpublished).
[34] R. L. Brown and W. Klemperer, J. Chem. Phys. **41**, 3072 (1964).
[35] J. I. Steinfeld and W. Klemperer, J. Chem. Phys. **42**, 3475 (1965).
[36] J. I. Steinfeld, J. Chem. Phys. **44**, 2740 (1966).
[37] J. E. Selwyn and J. I. Steinfeld, Chem. Phys. Lett. **4**, 217 (1969).
[38] J. Derouard and N. Sadeghi, Chem. Phys. Lett. **102**, 324 (1983).
[39] K. Nakagawa , M. Kitamura, K. Suzuki, T. Kondow, T. Munakata, and T. Kasuya, Chem. Phys. **106**, 259 (1986).
[40] J.-P. Nicolai and M. C. Heaven, J. Chem. Phys. **84**, 6694 (1986).